A spectral collocation method based on integrated Chebyshev polynomials for two-dimensional biharmonic boundary-value problems

N. Mai-Duy* and R.I. Tanner

School of Aerospace, Mechanical and Mechatronic Engineering

The University of Sydney, NSW 2006, Australia

Submitted to *Journal of Computational and Applied Mathematics*, 9th September 2005; revised 25th January 2006

*Corresponding author: Telephone +61 2 9351 7151, Fax +61 2 9351 7060, E-mail nam.maiduy@aeromech.usyd.edu.au

Abstract This paper reports a new spectral collocation method for numerically solving two-dimensional biharmonic boundary-value problems. The construction of the Chebyshev approximations is based on integration rather than conventional differentiation. This use of integration allows: (i) the imposition of the governing equation at the whole set of grid points including the boundary points and (ii) the straightforward implementation of multiple boundary conditions. The performance of the proposed method is investigated by considering several biharmonic problems of first and second kinds; more accurate results and higher convergence rates are achieved than with conventional differential methods.

Keywords: spectral collocation methods, biharmonic problems, multiple boundary conditions, integrated Chebyshev polynomials.

1 Introduction

Biharmonic problems arise in many applications such as in the analysis of fluid flow and thin-plate bending. Consider the biharmonic equation

$$\nabla^4 v = \frac{\partial^4 v}{\partial x^4} + 2\frac{\partial^4 v}{\partial x^2 \partial y^2} + \frac{\partial^4 v}{\partial y^4} = b(x, y) \tag{1}$$

on the square $-1 \leq x, y \leq 1$ subject to two types of boundary conditions

$$\{v,\ \frac{\partial^2 v}{\partial n^2}\} \quad \text{and} \tag{2}$$

$$\{v,\ \frac{\partial v}{\partial n}\} \tag{3}$$

where $b(x, y)$ is a known driving function and n is the direction normal to the boundary.

In the case of the second-kind biharmonic problem constituted by (1) and (2), one often prefers to split the governing equation (1) into a set of two weakly coupled Poisson

equations

$$\frac{\partial^2 v}{\partial x^2} + \frac{\partial^2 v}{\partial y^2} = u \tag{4}$$

$$\frac{\partial^2 u}{\partial x^2} + \frac{\partial^2 u}{\partial y^2} = b \tag{5}$$

in which each equation has its own boundary conditions. The solution procedure is thus straightforward: (i) to solve (5) for the variable u and (ii) to solve (4) for the variable v.

In the case of the first-kind biharmonic problem formed by (1) and (3), the solution procedure becomes complicated. The choice of the governing equation in the form between (4)-(5) and (1) has a profound effect on the computing strategy adopted. Using (4) and (5), one needs to derive a computational boundary condition for the new variable u, while using (1), one needs to deal with the multiple boundary conditions (two boundary conditions prescribed at each boundary point). The latter has the advantage of leading to a smaller system of algebraic equations for equivalent resolution.

Spectral methods have become increasingly popular in the computation of continuum mechanics problems. The main advantage of these methods lies in their accuracy for a given number of unknowns. For problems whose solutions are sufficiently smooth, they exhibit exponential rates of convergence/spectral accuracy. There are three most commonly used spectral versions, namely the Galerkin-type, tau and collocation methods. Among them, the spectral collocation/pseudospectral method is particularly attractive owing to its economy. Comprehensive discussions on spectral methods can be found in review articles and monographs, see for example [4,5,6,8,9,21,22,23,26].

There are relatively few papers on spectral methods for the direct solution of high-order problems. In the context of spectral collocation methods, there are two basic techniques to implementing the multiple boundary conditions. The first implements the multiple boundary conditions at the expense of leaving a number of interior points out of the

process of collocating the differential equation (e.g. [3,14,15]); here, it is referred to as the node-reduction technique (NRT). The second employs interpolants that satisfy the boundary conditions (e.g. [10,12,26,27]); here, it is referred to as the imposed-kernel technique (IKT). Both NRT and IKT are capable of giving very rapid convergence. The latter is more accurate; however, it is difficult to apply the technique to the case of nonhomogeneous boundary conditions.

Recently, in the context of the radial-basis-function (RBF) collocation method, it was found that the use of integration instead of conventional differentiation for constructing the RBF approximations enhances the quality of the approximation of derivatives and also provides an effective way to implement the multiple boundary conditions [18,20]. For the former, Kansa et al [13], Hernandez et al [11] and Ling and Trummer [16] made some discussions: since successively higher-order derivatives of the interpolants have their convergence rates reduced by the order of differentiation (Madych and Nelson [17], theorem 4.4), the use of integrated RBF expansions improves the reduction on the rate of convergence caused by the direct differentiation of the interpolants. For the latter, apart from the RBF coefficients, there are additional coefficients arising from the integration process which can be utilized to implement the multiple boundary conditions. There is thus no need to reduce the number of interior points used for discretizing the governing equation or to include the boundary conditions in the interpolants.

In this study, a spectral collocation method based on integrated Chebyshev polynomials for the solution of first- and second-kind biharmonic problems is proposed. Numerical results will show that the proposed method outperforms the conventional one in terms of accuracy and convergence rate, especially for the case of first-kind biharmonic problems.

The remainder of the paper is organized as follows. In section 2, Chebyshev spectral collocation methods based on the proposed integration and conventional differentiation formulations are presented. In section 3, the proposed method is verified through the

solution of the second-kind biharmonic problem governed by a set of two weakly coupled second-order equations and the first-kind biharmonic problem governed by a fourth-order equation. Section 4 gives some concluding remarks.

2 Chebyshev spectral collocation methods

The Chebyshev spectral collocation method can be described in the following way. An approximation based on Chebyshev polynomials to the variable v is first introduced. The set of collocation equations is then generated. The equation system consists of two parts. The first part is formed by making the associated residual, e.g. $(\nabla^4 v - b)$, equal to zero at the collocation points, while the second part is obtained by forcing the boundary conditions, e.g. v and $\partial v/\partial n$, to be satisfied at the boundary collocation points. These tasks need to be conducted in an appropriate manner and they will be presented in detail.

2.1 Chebyshev polynomials

The Chebyshev polynomial of first kind $T_k(x)$ is defined by

$$T_k(x) = \cos(k \arccos(x)) \qquad k = 0, 1, 2, \cdots \tag{6}$$

where $-1 \leq x \leq 1$. The polynomial $T_k(x)$ can be expanded in power series as

$$T_0(x) = 1 \tag{7}$$

$$T_k(x) = \frac{k}{2} \sum_{m=0}^{[k/2]} (-1)^m \frac{2^{k-2m}(k-m-1)!}{m!(k-2m)!} x^{k-2m}, \quad k > 0 \tag{8}$$

where $[k/2]$ is the integer part of $k/2$.

2.2 Conventional differentiation formulation (CDF)

Following standard procedures such as those by Trefethen [26], the conventional Chebyshev collocation method can be described as follows.

2.2.1 One-dimensional formulation

Consider a one-dimensional domain: $-1 \leq x \leq 1$ (Figure 1a). The domain of interest is discretized using the Gauss-Lobatto (G-L) points defined as

$$\{x_i\}_{i=0}^{N} = \left\{ \cos\left(\frac{\pi i}{N}\right) \right\}_{i=0}^{N}$$

An approximate solution v is sought in the truncated Chebyshev series form

$$v(x) = \sum_{k=0}^{N} a_k T_k(x) \tag{9}$$

where $\{a_k\}_{k=0}^{N}$ is the set of expansion coefficients to be found. The pth-order derivative of the variable v is then obtained through differentiation as

$$\frac{d^p v(x)}{dx^p} = \sum_{k=0}^{N} a_k \frac{d^p T_k(x)}{dx^p} \tag{10}$$

Apart from the capability to provide spectral accuracy, using the cosine-type points (9) also allows a fast Fourier transform to be used to convert the expansion coefficients $\{a_k\}_{k=0}^{N}$ (spectral space) into the nodal variable values $\{v(x_i)\}_{i=0}^{N}$ (physical space):

$$a_k = \frac{2}{N\bar{c}_k} \sum_{i=0}^{N} \frac{1}{\bar{c}_i} v_i T_k(x_i) \tag{11}$$

where $\bar{c}_0 = \bar{c}_N = 2,\ \bar{c}_i = 1$ for $i = 1, 2, \cdots, N-1$.

The values of the derivative $d^k v/dx^k$, with $k = (1, 2, \cdots, p)$, at the G-L points can be computed by

$$\widehat{\frac{dv}{dx}} = \mathcal{D}^{(1)}\widehat{v} = \mathcal{D}\widehat{v} \tag{12}$$

$$\widehat{\frac{d^2v}{dx^2}} = \mathcal{D}^{(2)}\widehat{v} = \mathcal{D}^2\widehat{v} \tag{13}$$

$$\cdots \quad \cdots \quad \cdots \quad \cdots$$

$$\widehat{\frac{d^pv}{dx^p}} = \mathcal{D}^{(p)}\widehat{v} = \mathcal{D}^p\widehat{v} \tag{14}$$

where $\widehat{\cdot}$ labels the vector, e.g., $\widehat{v} = (v(x_0), v(x_1), \cdots, v(x_N))^T$, and $\mathcal{D}^{(\cdot)}$ are the differentiation matrices. The entries of $\mathcal{D}$ ($\mathcal{D}^{(1)}$) are

$$\mathcal{D}_{ij} = \frac{\bar{c}_i}{\bar{c}_j}\frac{(-1)^{i+j}}{x_i - x_j}, \qquad 0 \le i, j \le N, \quad i \ne j \tag{15}$$

$$\mathcal{D}_{ii} = -\frac{x_i}{2(1 - x_i^2)}, \qquad 1 \le i \le N - 1 \tag{16}$$

$$\mathcal{D}_{11} = -\mathcal{D}_{NN} = \frac{2N^2 + 1}{6} \tag{17}$$

As an alternative approach, the diagonal entries of $\mathcal{D}$ can be computed in the way that represents exactly the derivative of a constant [2]

$$\mathcal{D}_{ii} = -\sum_{j=0, j\ne i}^{N} \mathcal{D}_{ij} \tag{18}$$

Higher-order derivatives $\mathcal{D}^{(p)}$ can be constructed using recursions, see for example [7,27,28], which are faster and more numerically stable. The roundoff properties of the spectral differentiation matrices were studied in, e.g., [1,2] and References therein.

Using (12)-(14), one can reduce ordinary differential equations to systems of algebraic equations. More details can be found in [26].

2.2.2 Two-dimensional formulation

Consider a two-dimensional domain: $-1 \leq x, y \leq 1$ (Figure 1b). The domain of interest is represented by a tensor product grid formed by the G-L points in each coordinate direction

$$\{x_i\}_{i=0}^{N_x} = \left\{ \cos\left(\frac{\pi i}{N_x}\right) \right\}_{i=0}^{N_x} \qquad \{y_j\}_{j=0}^{N_y} = \left\{ \cos\left(\frac{\pi j}{N_y}\right) \right\}_{j=0}^{N_y}$$

An approximate solution is sought in the polynomial $v(x, y)$ of degree at most equal to N_x and N_y in the $x-$ and $y-$directions, respectively. The Chebyshev approximations for derivatives over 2D grids can be constructed using the tensor product theory [26]. Two horizontal and vertical blocks are introduced here for the purpose of computing the derivatives with respect to x and y, respectively (Figure 1b). In each block, the grid points are numbered from bottom to top and from left to right. The discretized boundaries do not include the four corners of a square.

In the horizontal block, the values of relevant derivatives with respect to x at the grid points can be computed by

$$\begin{aligned} &\widehat{\frac{\partial v}{\partial x}} = \left(\mathcal{D}^{(1)} \otimes \mathbf{I}\right) \widehat{v}, \quad \widehat{\frac{\partial^2 v}{\partial x^2}} = \left(\mathcal{D}^{(2)} \otimes \mathbf{I}\right) \widehat{v}, \\ &\widehat{\frac{\partial^4 v}{\partial x^4}} = \left(\mathcal{D}^{(4)} \otimes \mathbf{I}\right) \widehat{v}, \quad \widehat{\frac{\partial^2}{\partial x^2}\left(\frac{\partial^2 v}{\partial y^2}\right)} = \left(\mathcal{D}^{(2)} \otimes \mathbf{I}\right) \widehat{\frac{\partial^2 v}{\partial y^2}} \end{aligned} \tag{19}$$

where $\mathcal{D}^{(.)}$ are the differentiation matrices of dimension $(N_x + 1) \times (N_x + 1)$ obtained from the one-dimensional case, $\mathbf{I}$ is the identity matrix of dimension $(N_y - 1) \times (N_y - 1)$, and $\otimes$ denotes the Kronecker tensor product (direct product). Using the values of the boundary condition v and its tangent derivative $\partial^2 v/\partial y^2$ at the boundary points along the two vertical lines, (19) is rewritten as

$$\begin{aligned} &\widehat{\frac{\partial v}{\partial x}} = \widetilde{\mathcal{D}}^{(1x)} \widehat{v}_{ip} + \widehat{k}^{(1x)}, \quad \widehat{\frac{\partial^2 v}{\partial x^2}} = \widetilde{\mathcal{D}}^{(2x)} \widehat{v}_{ip} + \widehat{k}^{(2x)}, \\ &\widehat{\frac{\partial^4 v}{\partial x^4}} = \widetilde{\mathcal{D}}^{(4x)} \widehat{v}_{ip} + \widehat{k}^{(4x)}, \quad \widehat{\frac{\partial^2}{\partial x^2}\left(\frac{\partial^2 v}{\partial y^2}\right)} = \widetilde{\mathcal{D}}^{(2xy)} \left(\widehat{\frac{\partial^2 v}{\partial y^2}}\right)_{ip} + \widehat{k}^{(2xy)} \end{aligned} \tag{20}$$

where $\widehat{v}_{ip}$ and $\left(\widehat{\frac{\partial^2 v}{\partial y^2}}\right)_{ip}$ are vectors of interior values, $\widetilde{\mathcal{D}}^{(.)}$ and $\widehat{k}^{(.)}$ are known matrices and vectors. For homogeneous boundary conditions, (20) is reduced to

$$\begin{aligned} \widehat{\frac{\partial v}{\partial x}} &= \widetilde{\mathcal{D}}^{(1x)}\widehat{v}_{ip}, \quad \widehat{\frac{\partial^2 v}{\partial x^2}} = \widetilde{\mathcal{D}}^{(2x)}\widehat{v}_{ip}, \\ \widehat{\frac{\partial^4 v}{\partial x^4}} &= \widetilde{\mathcal{D}}^{(4x)}\widehat{v}_{ip}, \quad \widehat{\frac{\partial^2}{\partial x^2}\left(\frac{\partial^2 v}{\partial y^2}\right)} = \widetilde{\mathcal{D}}^{(2xy)}\left(\widehat{\frac{\partial^2 v}{\partial y^2}}\right)_{ip} \end{aligned} \tag{21}$$

which are often used for the structural and vibration analysis of thin plates.

Similarly, in the vertical block, the values of relevant derivatives with respective to y at the grid points can be computed by

$$\begin{aligned} \widehat{\frac{\partial v}{\partial y}} &= \widetilde{\mathcal{D}}^{(1y)}\widehat{v}_{ip} + \widehat{k}^{(1y)}, \quad \widehat{\frac{\partial^2 v}{\partial y^2}} = \widetilde{\mathcal{D}}^{(2y)}\widehat{v}_{ip} + \widehat{k}^{(2y)}, \\ \widehat{\frac{\partial^4 v}{\partial y^4}} &= \widetilde{\mathcal{D}}^{(4y)}\widehat{v}_{ip} + \widehat{k}^{(4y)}, \quad \widehat{\frac{\partial^2}{\partial y^2}\left(\frac{\partial^2 v}{\partial x^2}\right)} = \widetilde{\mathcal{D}}^{(2yx)}\left(\widehat{\frac{\partial^2 v}{\partial x^2}}\right)_{ip} + \widehat{k}^{(2yx)} \end{aligned} \tag{22}$$

where the boundary condition v and its tangent derivative $\partial^2 v/\partial x^2$ at the boundary points along the two horizontal lines are transformed into $\widehat{k}^{(.)}$s.

Using the results $\widehat{\frac{\partial^2 v}{\partial y^2}}$ obtained from (22) and $\widehat{\frac{\partial^2 v}{\partial x^2}}$ obtained from (20), the mixed partial derivatives in (20) and (22) are expressed in terms of the values of v at the interior points as

$$\begin{aligned} \widehat{\frac{\partial^4 v}{\partial x^2 \partial y^2}} &= \widetilde{\mathcal{D}}^{(4xy)}\widehat{v}_{ip} + \widehat{k}^{(4xy)} \\ \widehat{\frac{\partial^4 v}{\partial y^2 \partial x^2}} &= \widetilde{\mathcal{D}}^{(4yx)}\widehat{v}_{ip} + \widehat{k}^{(4yx)} \end{aligned} \tag{23}$$

In solving the second-kind biharmonic problem, the imposition of (4) and (5) at the $(N_x-1)(N_y-1)$ interior points $(x_i, y_i),\ i = (1, 2, \cdots, N_x - 1),\ j = (1, 2, \cdots, N_y - 1)$ using (20) and (22) yields two sets of algebraic equations for the values of v and u at the interior points which are only weakly coupled. These systems can be solved separately using Gaussian elimination.

For the first-kind biharmonic problem, there are two boundary conditions prescribed at each boundary point. The multiple boundary conditions can be implemented using the NRT that was briefly reviewed earlier. Following the work of Karageorghis [14], the

governing equation (1) is collocated at the $(N_x-3)(N_y-3)$ interior points (x_i, y_i), $i = (2, 3, \cdots, N_x-2)$, $j = (2, 3, \cdots, N_y-2)$. Along the two vertical lines, the normal derivative boundary conditions $\partial v/\partial n$ are imposed at the $2(N_y-1)$ boundary points $bx1$ and $bx2$; along the two horizontal lines, they are imposed at the $2(N_x-3)$ interior points of $by1$ and $by2$. This leads to a set of $(N_x-1)(N_y-1)$ equations in $(N_x-1)(N_y-1)$ unknowns

$$\left(\widetilde{\mathcal{D}}^{(4x)}+\widetilde{\mathcal{D}}^{(4xy)}+\widetilde{\mathcal{D}}^{(4yx)}+\widetilde{\mathcal{D}}^{(4y)}\right)_{ip^*}\widehat{v}_{ip}=\left(\widehat{b}-\widehat{k}^{(4x)}-\widehat{k}^{(4xy)}-\widehat{k}^{(4yx)}-\widehat{k}^{(4y)}\right)_{ip^*} \tag{24}$$

$$\widetilde{\mathcal{D}}^{(1x)}_{bx1,bx2}\widehat{v}_{ip}=\left(\widehat{\frac{\partial v}{\partial x}}\right)_{bx1,bx2}-\widehat{k}^{(1x)}_{bx1,bx2} \tag{25}$$

$$\widetilde{\mathcal{D}}^{(1y)}_{by1^*,by2^*}\widehat{v}_{ip}=\left(\widehat{\frac{\partial v}{\partial y}}\right)_{by1^*,by2^*}-\widehat{k}^{(1y)}_{by1^*,by2^*} \tag{26}$$

where $ip^* \subset ip$, $by1^* \subset by1$, $by2^* \subset by2$ (as defined above). The resulting algebraic system can be solved using Gaussian elimination.

As an alternative approach, the multiple boundary conditions can be imposed using the IKT (the interpolants satisfy the boundary conditions). For example, in the analysis of clamped thin-plate problems, one can first multiply interpolating polynomials by $(1-x^2)$ and $(1-y^2)$ and then delete appropriate numbers of columns and rows of the system matrix. More details can be found in [26,27], where MATLAB software packages implementing pseudospectral methods are also provided.

2.3 Proposed integration formulation (PIF)

The Chebyshev expressions representing the dependent variable and its derivatives in the governing equation are constructed through integration instead of conventional differentiation. This use of integration produces additional coefficients (integration constants) that can be utilized for the purpose of forcing the multiple boundary conditions as well as the

differential equation on the boundaries. (The detailed implementation of the collocation formulation based on integration using radial basis functions for the direct solution of high-order differential equations was reported in [18,20].)

2.3.1 One-dimensional formulation

Consider a one-dimensional domain, $-1 \leq x \leq 1$. The domain is discretized using the G-L points (Figure 1a). Since the construction process of the PIF starts with the approximation of a derivative rather than with the approximation of its original function, it may have many eligible starting points. For this reason, a scheme order is introduced here. The pth-order PIF scheme, denoted by PIF-p, is an approximation scheme in which the pth-order derivative is first sought in the truncated Chebyshev series form and then integrated p times to obtain expressions for lower-order derivatives and the function itself

$$\frac{d^p v(x)}{dx^p} = \sum_{k=0}^{N} a_k T_k(x) = \sum_{k=0}^{N} a_k I_k^{(p)}(x) \tag{27}$$

$$\frac{d^{p-1} v(x)}{dx^{p-1}} = \sum_{k=0}^{N} a_k I_k^{(p-1)}(x) + c_1 \tag{28}$$

$$\frac{d^{p-2} v(x)}{dx^{p-2}} = \sum_{k=0}^{N} a_k I_k^{(p-2)}(x) + c_1 x + c_2 \tag{29}$$

$$\cdots \quad \cdots \qquad \cdots \qquad \cdots \qquad \cdots$$

$$\frac{dv(x)}{dx} = \sum_{k=0}^{N} a_k I_k^{(1)}(x) + c_1 \frac{x^{p-2}}{(p-2)!} + c_2 \frac{x^{p-3}}{(p-3)!} + \cdots + c_{p-2} x + c_{p-1} \tag{30}$$

$$v(x) = \sum_{k=0}^{N} a_k I_k^{(0)}(x) + c_1 \frac{x^{p-1}}{(p-1)!} + c_2 \frac{x^{p-2}}{(p-2)!} + \cdots + c_{p-1} x + c_p \tag{31}$$

where $I_k^{(p-1)}(x) = \int I_k^{(p)}(x)dx,\ I_k^{(p-2)}(x) = \int I_k^{(p-1)}(x)dx, \cdots, I_k^{(0)}(x) = \int I_k^{(1)}(x)dx$. These integrals can be determined by using recurrence relations [23]

$$\int T_0(x)dx = T_1(x) \tag{32}$$

$$\int T_1(x)dx = \frac{1}{4}\left[T_0(x) + T_2(x)\right] \tag{33}$$

$$\int T_k(x)dx = \frac{1}{2}\left[\frac{T_{k+1}(x)}{(k+1)} - \frac{T_{k-1}(x)}{(k-1)}\right], \qquad k > 1 \tag{34}$$

or integrating (7)-(8) directly, e.g., for $k > 0$:

$$I_k^{(p-1)}(x) = \int T_k(x)dx = \frac{k}{2}\sum_{m=0}^{[k/2]}(-1)^m \frac{2^{k-2m}(k-m-1)!}{m!(k-2m+1)!}x^{k-2m+1} \tag{35}$$

$$I_k^{(p-2)}(x) = \int I_k^{(p-1)}(x)dx = \frac{k}{2}\sum_{m=0}^{[k/2]}(-1)^m \frac{2^{k-2m}(k-m-1)!}{m!(k-2m+2)!}x^{k-2m+2} \tag{36}$$

$$\cdots \quad \cdots \qquad \cdots \qquad \cdots \qquad \cdots$$

$$I_k^{(0)}(x) = \int I_k^{(1)}(x)dx = \frac{k}{2}\sum_{m=0}^{[k/2]}(-1)^m \frac{2^{k-2m}(k-m-1)!}{m!(k-2m+p)!}x^{k-2m+p} \tag{37}$$

The evaluation of (27)-(31) at the G-L points leads to

$$\widehat{\frac{d^p v}{dx^p}} = \mathcal{I}^{(p)}\widehat{s} \tag{38}$$

$$\widehat{\frac{d^{p-1} v}{dx^{p-1}}} = \mathcal{I}^{(p-1)}\widehat{s} \tag{39}$$

$$\cdots \quad \cdots \quad \cdots$$

$$\widehat{\frac{dv}{dx}} = \mathcal{I}^{(1)}\widehat{s} \tag{40}$$

$$\widehat{v} = \mathcal{I}^{(0)}\widehat{s} \tag{41}$$

where $\mathcal{I}^{(p)}, \mathcal{I}^{(p-1)}, \cdots, \mathcal{I}^{(0)}$ are the integration matrices and $\widehat{s} = (a_0, a_1, \cdots, a_N, c_1, c_2, \cdots, c_p)^T$. For convenience of computation, $\mathcal{I}^{(p)}, \mathcal{I}^{(p-1)}, \cdots, \mathcal{I}^{(1)}$ are augmented using zero-submatrices so that they have the same dimension as $\mathcal{I}^{(0)}$.

Phillips and Karageorghis [24] employed integrated expansions of ultraspherical polynomials, of which the Chebyshev and Legendre polynomials are important special cases, for solving one-dimensional linear constant-coefficient second-order boundary-value problems. The differential equation is integrated twice; formulae relating the coefficients in the integrated expansions to those of the original expansion are proved. It is different from that method, the proposed integrated-expansion method is based on a collocation scheme. The differential equation is not integrated; integration is only used for the construct of the approximations. For the purpose of illustration, the present method is described in detail for the solution of a simple ordinary differential equation, namely $d^4v(x)/dx = b(x)$, subject to Dirichlet boundary conditions: $v(x_0) = \alpha, dv(x_0)/dx = \overline{\alpha}, v(x_N) = \beta$ and $dv(x_N)/dx = \overline{\beta}$. Using PIF-4, one can obtain the following square system of algebraic equations

$$\sum_{k=0}^{N} a_k I_k^{(4)}(x_0) + 0c_1 + 0c_2 + 0c_3 + 0c_4 = b(x_0) \tag{42}$$

$$\sum_{k=0}^{N} a_k I_k^{(4)}(x_1) + 0c_1 + 0c_2 + 0c_3 + 0c_4 = b(x_1) \tag{43}$$

$$\cdots \quad \cdots \quad \cdots \quad \cdots \quad \cdots \quad \cdots$$

$$\sum_{k=0}^{N} a_k I_k^{(4)}(x_N) + 0c_1 + 0c_2 + 0c_3 + 0c_4 = b(x_N) \tag{44}$$

$$\sum_{k=0}^{N} a_k I_k^{(0)}(x_0) + \frac{x_0^3}{6}c_1 + \frac{x_0^2}{2}c_2 + x_0c_3 + c_4 = \alpha \tag{45}$$

$$\sum_{k=0}^{N} a_k I_k^{(1)}(x_0) + \frac{x_0^2}{2}c_1 + x_0c_2 + c_3 + 0c_4 = \overline{\alpha} \tag{46}$$

$$\sum_{k=0}^{N} a_k I_k^{(0)}(x_N) + \frac{x_N^3}{6}c_1 + \frac{x_N^2}{2}c_2 + x_Nc_3 + c_4 = \beta \tag{47}$$

$$\sum_{k=0}^{N} a_k I_k^{(1)}(x_N) + \frac{x_N^2}{2}c_1 + x_Nc_2 + c_3 + 0c_4 = \overline{\beta} \tag{48}$$

for the unknown vector $(a_0, a_1, \cdots, a_N, c_1, c_2, c_3, c_4)^T$, in which the first $(N+1)$ equations are used for collocating the differential equation and the last 4 equations are employed

for imposing the boundary conditions. The accuracy of the proposed method for solving high-order ordinary differential equations was reported in [19]. This study is concerned with two-dimensional biharmmonic equations. One distinguishing feature of the two-dimensional formulation over the one-dimensional formulation is that the spectral coefficients are converted into the nodal variable values.

2.3.2 Two-dimensional formulation

Consider a two-dimensional domain, $-1 \leq x, y \leq 1$. The domain is represented through a tensor product grid (Figure 1b). As with the CDF case, two horizontal and vertical blocks are formed for computing the derivatives with respect to the $x-$ and $y-$directions, respectively (Figure 1b). The solution procedure involves the following steps

(i) To transform the spectral coefficients $\{s_i\}_{i=0}^{N+p}$ into the nodal variable values $\{v_i\}_{i=0}^{N}$. Here, it is referred to as a conversion process.
(ii) To use Kronecker products as usual to construct the approximations for derivatives over a tensor product grid of the horizontal and vertical blocks.
(iii) To compute the mixed partial derivatives over a grid using the relevant results of the horizontal and vertical blocks obtained from step (ii).
(iv) To discretize the governing equation at the interior points.
(v) To solve the obtained system of algebraic equations.

The most important difference between the two formulations occurs at step (i). For the PIF case, the set of unknown coefficients becomes larger owing to the presence of integration constants. It thus allows one to add additional equations to the conversion system. These extra equations will be exploited to impose the governing equation on the boundaries for the case of second-order equations (single boundary condition), and the governing equation on the boundaries together with normal derivative boundary conditions for the case of fourth-order equations (multiple boundary conditions). It is noted that these

conversion processes need to be carried out numerically because no such a fast Fourier transform algorithm is available here. Other steps (ii)-(v) in the above flowchart are similar to those of the CDF case and therefore, they are omitted here (the matrix-vector forms of the CFD case can be used here by simply replacing $\mathcal{D}$ with $\mathcal{I}$).

For step (i), only conversion processes in the horizontal block ($x-$direction) are described in detail here (those in the vertical block ($y-$direction) are conducted in the same manner). To simplify the notation, subscripts x will be dropped.

As mentioned earlier, the PIF-p scheme permits one to approximate a function and its derivatives of orders up to p. The scheme order p should be chosen to be less than or equal to the order of the differential equation. In solving the first-kind biharmonic problems governed by a fourth-order equation, the PIF-4 scheme is employed to represent the derivatives $\partial^4 v/\partial x^4$ and $\partial^4 v/\partial y^4$, while the PIF-2 scheme is utilized for computing the mixed partial derivatives according to

$$\frac{\partial^4 v}{\partial x^2 \partial y^2} = \frac{\partial^2}{\partial x^2}\left(\frac{\partial^2 v}{\partial y^2}\right) \quad \text{and} \quad \frac{\partial^4 v}{\partial y^2 \partial x^2} = \frac{\partial^2}{\partial y^2}\left(\frac{\partial^2 v}{\partial x^2}\right)$$

In solving the second-kind biharmonic problem governed by a set of two second-order equations, all derivatives are approximated using the PIF-2 scheme.

Along each line in a tensor product grid (one-dimensional domain), the PIF-2 scheme

leads to

$$
\begin{aligned}
v_0 &= \sum_{k=0}^{N} a_k I_k^{(2)}(x_0) + x_0 c_1 + c_2 \\
&\cdots \quad \cdots \quad \cdots \\
v_N &= \sum_{k=0}^{N} a_k I_k^{(2)}(x_N) + x_N c_1 + c_2 \\
f_1 &= \sum_{k=0}^{N} a_k I_k^{(\alpha)}(x_0) + \alpha_1 c_1 + \alpha_2 c_2 \\
f_2 &= \sum_{k=0}^{N} a_k I_k^{(\beta)}(x_N) + \beta_1 c_1 + \beta_2 c_2
\end{aligned}
\tag{49}
$$

while the PIF-4 scheme results in

$$
\begin{aligned}
v_0 &= \sum_{k=0}^{N} a_k I_k^{(4)}(x_0) + \frac{x_0^3}{6} c_1 + \frac{x_0^2}{2} c_2 + x_0 c_3 + c_4 \\
&\cdots \quad \cdots \quad \cdots \quad \cdots \quad \cdots \\
v_N &= \sum_{k=0}^{N} a_k I_k^{(4)}(x_N) + \frac{x_N^3}{6} c_1 + \frac{x_N^2}{2} c_2 + x_N c_3 + c_4 \\
f_1 &= \sum_{k=0}^{N} a_k I_k^{(\alpha)}(x_0) + \alpha_1 c_1 + \alpha_2 c_2 + \alpha_3 c_3 + \alpha_4 c_4 \\
f_2 &= \sum_{k=0}^{N} a_k I_k^{(\beta)}(x_N) + \beta_1 c_1 + \beta_2 c_2 + \beta_3 c_3 + \beta_4 c_4 \\
f_3 &= \sum_{k=0}^{N} a_k I_k^{(\gamma)}(x_0) + \gamma_1 c_1 + \gamma_2 c_2 + \gamma_3 c_3 + \gamma_4 c_4 \\
f_4 &= \sum_{k=0}^{N} a_k I_k^{(\theta)}(x_N) + \theta_1 c_1 + \theta_2 c_2 + \theta_3 c_3 + \theta_4 c_4
\end{aligned}
\tag{50}
$$

where the last two equations in (49) and the last four equations in (50) are additional equations representing 'extra information' f_i. Tables 1 and 2 present in detail the information f_i used for computing $\partial^2 v/\partial x^2$ in the solution of (4), and $\partial^2 v/\partial x^2$, $\partial^4 v/\partial x^4$ and $\partial^4 v/\partial x^2 \partial y^2$ in the solution of (1), respectively.

Since the two systems (49) and (50) have similar structures, it is convenient to write them in the following matrix-vector form

$$\left\{ \begin{array}{c} \widehat{v} \\ \widehat{f} \end{array} \right\} = \mathcal{C} \left\{ \begin{array}{c} \widehat{a} \\ \widehat{c} \end{array} \right\} = \mathcal{C}\widehat{s} \tag{51}$$

where $\mathcal{C}$ is the conversion matrix. The dimensions of $\mathcal{C}$ and $\widehat{f}$ are $(N+3) \times (N+3)$ and 2×1 for the PIF-2 scheme, and $(N+5) \times (N+5)$ and 4×1 for the PIF-4 scheme, respectively. Solving (51) yields

$$\widehat{s} = \mathcal{C}^{-1} \left\{ \begin{array}{c} \widehat{v} \\ \widehat{f} \end{array} \right\} \tag{52}$$

Substitution of (52) into (38)-(40) leads to

$$\begin{array}{l} \widehat{\dfrac{d^p v}{dx^p}} = \mathcal{I}^{(p)} \mathcal{C}^{-1} \left\{ \begin{array}{c} \widehat{v} \\ \widehat{f} \end{array} \right\} \\ \cdots \quad \cdots \quad \cdots\cdots \quad \cdots \\ \widehat{\dfrac{dv}{dx}} = \mathcal{I}^{(1)} \mathcal{C}^{-1} \left\{ \begin{array}{c} \widehat{v} \\ \widehat{f} \end{array} \right\} \end{array} \tag{53}$$

where $p \leq 2$ for PIF-2 and $p \leq 4$ for PIF-4. Expressions (53) can be rewritten as

$$\begin{array}{l} \widehat{\dfrac{d^p v}{dx^p}} = \widetilde{\mathcal{I}}^{(p)} \widehat{v} + \widehat{h}^{(p)} \\ \cdots \quad \cdots \quad \cdots \\ \widehat{\dfrac{dv}{dx}} = \widetilde{\mathcal{I}}^{(1)} \widehat{v} + \widehat{h}^{(1)} \end{array} \tag{54}$$

where $\widetilde{\mathcal{I}}^{(.)}$ and $\widehat{h}^{(.)}$ are known matrices and vectors. It is noted that the vectors $\widehat{f}$ on the right-hand side of (53) involve terms which are given (e.g., known driving functions and boundary conditions) or easily computed (tangent derivatives of boundary conditions),

except for the special term

$$\frac{\partial^2}{\partial x^2}\left(\frac{\partial^2 v}{\partial y^2}\right)$$

at the two end points. The values of this term at the collocation points are not known so that one needs to use its expression (a sum of the nodal variable values) instead. Hence, it will be inserted back into the integration matrix $\left(\mathcal{I}^{(.)}\mathcal{C}^{-1}\right)$ via the last two columns.

After performing steps (i), (ii) and (iii), the boundary conditions are incorporated into the approximations. Furthermore, the governing equation is forced to be satisfied exactly at the boundary points bx_1, bx_2, by_1 and by_2. As a result, step (iv) is then used for collocating the governing equations at the interior points only. The obtained system can be solved using Gaussian elimination for the nodal variable values.

For a given N, although the PIF case involves an additional algebraic polynomial of degree equal to 3 for PIF-4 and 1 for PIF-2, it still requires exactly the same discretization (mesh size) as the CDF case in seeking the approximate solution in terms of nodal variable values. Furthermore, the system matrix obtained by PIF has the same dimension as that yielded through CDF.

For the CDF case, the question here is how it works when an algebraic polynomial is added to (9) in order to have "the same form" as the PIF case, i.e.,

$$v(x) = \sum_{k=0}^{N} a_k T_k(x) + c_1 \frac{x^{p-1}}{(p-1)!} + c_2 \frac{x^{p-2}}{(p-2)!} + \cdots c_{p-1}x + c_p \tag{55}$$

It can be seen that a set of polynomials $\left(\{T_k\}_{k=0}^{N}, \frac{x^{p-1}}{(p-1)!}, \cdots, x, 1\right)$ in (55) is not linearly independent because the first and last two polynomials are identical. Consequently, it cannot further proceed with the same treatment of multiple boundary conditions as for the PIF case.

The proposed formulation provides an effective way to implement the multiple boundary

conditions. However, it requires more work to construct 1-D Chebyshev approximations largely because of the need for a numerical conversion of spectral space (the coefficients) into physical space (the grid values). Fortunately, these calculations are conducted in one-dimensional domains only, and hence they do not add greatly to the computational cost.

3 Numerical results

Several biharmonic boundary-value problems including the static analysis of thin-plate are considered in this section to investigate the performance of the proposed method. A rigorous discussion of thin-plate problems is available in many texts, see, e.g., [25]. The results obtained by CDF are also presented for comparison. The accuracy of a numerical solution produced by an approximate scheme is measured via the norm of relative errors of the solution

$$N_e(\phi) = \sqrt{\frac{\sum_{i=1}^{n_{ip}} \left(\phi_i^{(e)} - \phi_i\right)^2}{\sum_{i=1}^{n_{ip}} \left(\phi_i^{(e)}\right)^2}} \tag{56}$$

where n_{ip} is the number of interior points, $\phi_i^{(e)}$ and ϕ_i are the exact and computed values of the solution ϕ at point i. Another important measure is the order of the accuracy defined by

$$N_e(N) \approx \gamma \left(\frac{1}{N}\right)^{\theta} = O(N^{-\theta}) \tag{57}$$

where γ and θ are the exponential model's parameters. Given a set of observations, these parameters can be found by the general linear least squares technique.

3.1 Problem 1: simply-supported square-thin-plate

Consider a simply-supported square-thin-plate ($-1 \leq x, y \leq 1$) under the action of a distributed loading of the form

$$b(x, y) = 4 \sin(\pi x) \sin(\pi y) \tag{58}$$

The boundary conditions for the simply-supported plate [25] are

$$v = 0 \quad \text{and} \quad \frac{\partial^2 v}{\partial n^2} = 0$$

This problem can be solved analytically and the exact solution for the deflection is

$$v^{(e)}(x, y) = \frac{1}{\pi^4} \sin(\pi x) \sin(\pi y) \tag{59}$$

which is plotted in Figure 2. This is a biharmonic boundary-value problem of second kind. The governing equation (1) is split into two Poisson equations (4) and (5) with Dirichlet boundary conditions. Several tensor product grids are employed to study the behaviour of convergence. The obtained results concerning the conditioning of the system matrix, the error norms of the solutions v and u, and the order of the accuracy are presented in Table 3. The condition numbers evaluated here are in 2-norm, the ratio of the largest singular value of the system matrix to the smallest. It can be seen that both formulations converge at exponential rates. The orders of N_e of the solution u for the first five sets are $O(N^{-19.24})$ and $O(N^{-17.38})$ for PIF and CDF, respectively; the proposed formulation provides faster convergence. In terms of accuracy, the PIF case yields more accurate results than the CDF case for all grids employed. For example, the errors $N_e(u)$ and $N_e(v)$ at a grid of 10×10 are 7.19×10^{-7} and 9.84×10^{-7} for PIF, and 1.02×10^{-5} and 1.30×10^{-5} for CDF, respectively. For finer grids of 18×18 and 20×20, their errors are extremely small (not exactly zero due to rounding errors on the computer). In terms of

the conditioning of the system, the proposed formulation leads to matrices with slightly lower condition numbers than those which arise in the conventional one.

3.2 Problem 2: clamped square-thin-plate

A square thin-plate ($-1 \leq x, y \leq 1$) with built-in edges is considered. The boundary conditions for the clamped thin-plate [25] are

$$v = 0 \quad \text{and} \quad \frac{\partial v}{\partial n} = 0$$

Given the following load distribution

$$b(x, y) = 4\cos(\pi x)\cos(\pi y) + \cos(\pi x) + \cos(\pi y) \tag{60}$$

the exact solution for the deflection can be verified to be

$$v^{(e)}(x, y) = \frac{1}{\pi^4}\left[1 + \cos(\pi x)\right]\left[1 + \cos(\pi y)\right] \tag{61}$$

which is plotted in Figure 3. This is a biharmonic problem of first-kind. In the present work, the governing equation (1) is solved directly, i.e. without splitting it into two Poisson equations. For the CDF case, the NRT and IKT are both employed to implement the multiple boundary conditions. The obtained results concerning the conditioning of the system matrix, the error norm of the solution v, and the order of the accuracy are presented in Table 4. The PIF approach yields the most accurate results, followed by IKT and then by NRT. For example, using a grid of 12×12, N_es are 5.27×10^{-9}, 3.80×10^{-8} and 2.24×10^{-5}, respectively. Furthermore, the proposed approach produces faster convergence. For the first five grids, the three approaches PIF, IKT and NRT converge apparently as $O(N^{-21.10})$, $O(N^{-19.13})$ and $O(N^{-13.36})$, respectively. The results obtained by NRT are far less accurate (almost three orders of magnitudes higher) and their conver-

gence is much slower than the others, probably due to the fact that this technique does not collocate the governing equation at every interior point. The conditioning numbers which arise in the PIF case are slightly less than those yielded through the CDF case.

3.3 Problem 3: Boundary conditions of complicated shapes

The purpose of giving this example here is to further verify the proposed method for cases, where the prescribed boundary conditions v and $\partial v/\partial n$ are of complicated shapes (non-homogeneous boundary conditions). Consider a square domain $-1 \leq x, y \leq 1$. The driving function is given by

$$b(x,y) = 16(\pi^2 - 1)^2 \left[\sin(2\pi x)\cosh(2y) - \cos(2\pi x)\sinh(2y)\right] \tag{62}$$

and the prescribed boundary conditions are

$$v = -\sinh(2y) \tag{63}$$

$$\frac{\partial v}{\partial x} = 2\pi\cosh(2y) \tag{64}$$

along the two vertical lines and

$$v = \sin(2\pi x)\cosh(\pm 2) - \cos(2\pi x)\sinh(\pm 2) \tag{65}$$

$$\frac{\partial v}{\partial y} = 2\left[\sin(2\pi x)\sinh(\pm 2) - \cos(2\pi x)\cosh(\pm 2)\right] \tag{66}$$

along the two horizontal lines. The exact solution can be found as

$$v^{(e)}(x,y) = \sin(2\pi x)\cosh(2y) - \cos(2\pi x)\sinh(2y) \tag{67}$$

The plot of (67) is shown in Figure 4. Unlike clamped thin-plate bending problems, all boundary data here are non-zero. It is difficult to apply the IKT to this problem; only the

NRT is employed here. Results concerning the error norm of the solution v obtained by PIF and CDF are shown in Tables 5, where similar remarks can be made as for thin-plate bending problems.

By regarding the results of the CDF case for low- and high-order equations as the basis, it can be seen that the performance of PIF is enhanced with increasing order of the differential equation. For example, the value difference of θ in $O(N^{-\theta})$ between the two formulations is about 2 for Poisson equations (Table 3), but up to about 5 for biharmonic equations (Table 5). The proposed method appears to be particularly well suited to high-order equations with non-homogeneous boundary conditions.

One important result here is the PIF yields faster convergence with respect to mesh refinement than the CDF. From the literature, it has been shown that successively higher derivatives of the interpolants have their convergence rates reduced by the order of differentiation (e.g., Madych and Nelson [17], theorem 4.4, page 226 for RBFs; Trefethen [26], theorem 4, page 34). Here, we have also numerically investigated the order of accuracy of the Chebyshev collocation scheme for the approximation of a function and its derivatives. Consider a function $y = \sin(\pi x)$, $-1 \leq x \leq 1$. Using $N = (6, 8, \cdots, 22)$, the convergence rates obtained are of $O(N^{-24.82}), O(N^{-23.40}), O(N^{-21.48})$ and $O(N^{-19.61})$ for the approximation of the first-, second-, third- and fourth-order derivatives, respectively. It can be seen that the convergence rate is a decreasing function of the order of the derivative. It appears that the use of integration, which is a smoothing operation, to construct the Chebyshev approximations improves the reduction on the rate of convergence caused by the direct differentiation of the interpolants, and it also provides a more effective way to implement the multiple boundary conditions. These are the main distinguishing features of the proposed method. It should be emphasized that all comparisons of accuracy and convergence rate between the proposed and conventional methods are based on the same discretizations ("mesh size").

4 Concluding remarks

This paper reports a spectral collocation method based on integrated Chebyshev polynomials for numerically solving biharmonic boundary-value problems. The use of integration to construct the approximations allows the multiple boundary conditions to be incorporated more efficiently. The governing equations are also forced to be satisfied exactly at the boundary points through the process of converting spectral space into physical space. Apart from the conversion process, the proposed and conventional methods can be implemented in a similar fashion. For a given N, the proposed method employs exactly the same spectral tensor product grid and this leads to a system matrix of the same dimension. Numerical results show that its performance is superior to those of the conventional methods regarding accuracy and convergence rate. We believe that the proposed method is applicable to higher-order partial differential equations and to other sets of orthogonal polynomials.

Acknowledgements N. Mai-Duy wishes to thank the University of Sydney for a Sesquicentennial Postdoctoral Research Fellowship. We would like to thank the referees for their comments to improve the paper.

References

1. R. Baltensperger and M.R. Trummer, Spectral differencing with a twist, *SIAM Journal on Scientific Computing* **24** (2003) 1465–1487.

2. A. Bayliss, A. Class and B.J. Matkowsky, Roundoff error in computing derivatives using the Chebyshev differentiation matrix, *Journal of Computational Physics* **116** (1995) 380–383.

3. C. Bernardi, G. Coppoletta and Y. Maday, Some spectral approximations of two-dimensional fourth-order problems, *Mathematics of Computation* **59** (1992) 63–76.

4. C. Bernardi and Y. Maday, Spectral methods. In: P.G. Ciarlet and J.L. Lions (Ed.) *Handbook of Numerical Analysis, Vol 5*, Elsevier Science, North Holland, 1997, pp. 209–485.

5. J.P. Boyd, *Chebyshev and Fourier Spectral Methods*, Dover, New York, 2001.

6. C. Canuto, M.Y. Hussaini, A. Quarteroni and T.A. Zang, *Spectral Methods in Fluid Dynamics*, Springer-Verlag, New York, 1988.

7. B. Fornberg, Generation of finite difference formulas on arbitrarily spaced grids, *Mathematics of Computation* **51** (1988) 699-706.

8. B. Fornberg, *A Practical Guide to Pseudospectral Methods*, Cambridge University Press, Cambridge, 1998.

9. D. Gottlieb and S.A. Orszag, *Numerical Analysis of Spectral Methods: Theory and Applications*, SIAM, Philadelphia, 1977.

10. W. Heinrichs, A spectral multigrid method for the Stokes problem in streamfunction formulation, *Journal of Computational Physics* **102** (1992) 310–318.

11. A. Hernandez Rosales, A. La Rocca and H. Power, Radial basis function Hermite collocation approach for the numerical simulation of the effect of precipitation inhibitor on the crystallization process of an over-saturated solution, *Numerical Methods for Partial Differential Equations*, **22** (2006) 361–380.

12. W. Huang and D.M. Sloan, The pseudospectral method for solving differential eigenvalue problems, *Journal of Computational Physics* **111** (1994) 399–409.

13. E.J. Kansa, H. Power, G.E. Fasshauer and L. Ling, A volumetric integral radial basis function method for time-dependent partial differential equations: I. Formulation, *Engineering Analysis with Boundary Elements*, **28** (2004) 1191–1206.

14. A. Karageorghis, A note on the satisfaction of the boundary conditions for Chebyshev collocation methods in rectangular domains, *Journal of Scientific Computing* **6** (1991) 21–26.

15. A. Karageorghis, Satisfaction of boundary conditions for Chebyshev collocation methods in cuboidal domains, *Computers & Mathematics with Applications* **27** (1994) 85–90.

16. L. Ling and M.R. Trummer, Multiquadric collocation method with integralformulation for boundary layer problems, *Computers & Mathematics with Applications*, **48**(5–6) (2004) 927–941.

17. W.R. Madych and S.A. Nelson, Multivariate interpolation and conditionally positive definite functions, II, *Mathematics of Computation*, **54**(189) (1990) 211–230.

18. N. Mai-Duy, Solving high order ordinary differential equations with radial basis function networks, *International Journal for Numerical Methods in Engineering* **62** (2005) 824–852.

19. N. Mai-Duy, An effective spectral collocation method for the direct solution of high-order ODEs, *Communications in Numerical Methods in Engineering*, in press.

20. N. Mai-Duy and R.I. Tanner, Solving high order partial differential equations with radial basis function networks, *International Journal for Numerical Methods in Engineering* **63**(2005) 1636–1654.

21. J.C. Mason and D.C. Handscomb, *Chebyshev Polynomials*, Chapman and Hall/CRC, Boca Raton, 2003.

22. J.C. Mason and T.N. Phillips (Guest Editors), *Numerial Algorithms, Volume 38, Number 1, Chebyshev Polynomials and Spectral Methods*, 2005.

23. R. Peyret, *Spectral Methods for Incompressible Viscous Flow*, Springer-Verlag, New York, 2002.

24. T.N. Phillips and A. Karageorghis, On the coefficients of integrated expansions of ultraspherical polynomials, *SIAM Journal on Numerical Analysis* **27**(3) (1990) 823–830.

25. S. Timoshenko and S. Woinowsky-Krieger, *Theory of Plates and Shells*, McGraw-Hill, New York, 1959.

26. L.N. Trefethen, *Spectral Methods in MATLAB*, SIAM, Philadelphia, 2000.

27. J.A.C. Weideman and S.C. Reddy, A MATLAB differentiation matrix suite, *ACM Transactions on Mathematical Software* **26** (2000) 465–519.

28. B.D. Welfert, Generation of pseudospectral differentiation matrices I, *SIAM Journal on Numerical Analysis* **34** (1997) 1640–1657.

Table 1: $\nabla^2 v = u$: extra information used for constructing a conversion matrix

Term	Scheme	Extra information
$\frac{\partial^2 v}{\partial x^2}$	PIF-2	$f_1 = \frac{\partial^2 v}{\partial x^2}(x_0) = b(x_0) - \frac{\partial^2 v}{\partial y^2}(x_0)$
		$f_2 = \frac{\partial^2 v}{\partial x^2}(x_N) = b(x_N) - \frac{\partial^2 v}{\partial y^2}(x_N)$

Table 2: $\nabla^4 v = b$: extra information used for constructing a conversion matrix

Term	Scheme	Extra information
$\frac{\partial^2 v}{\partial x^2}$	PIF-2	$f_1 = \frac{\partial v}{\partial x}(x_0)$ $f_2 = \frac{\partial v}{\partial x}(x_N)$
$\frac{\partial^2}{\partial x^2}\left(\frac{\partial^2 v}{\partial y^2}\right)$	PIF-2	$f_1 = \frac{\partial}{\partial x}\left(\frac{\partial^2 v}{\partial y^2}\right)(x_0) = \frac{\partial^2}{\partial y^2}\left(\frac{\partial v}{\partial x}\right)(x_0)$ $f_2 = \frac{\partial}{\partial x}\left(\frac{\partial^2 v}{\partial y^2}\right)(x_N) = \frac{\partial^2}{\partial y^2}\left(\frac{\partial v}{\partial x}\right)(x_N)$
$\frac{\partial^4 v}{\partial x^4}$	PIF-4	$f_1 = \frac{\partial v}{\partial x}(x_0)$ $f_2 = \frac{\partial v}{\partial x}(x_N)$ $f_3 = \frac{\partial^4 v}{\partial x^4}(x_0) = b(x_0) - \frac{\partial^4 v}{\partial y^4}(x_0) - 2\frac{\partial^2}{\partial x^2}\left(\frac{\partial^2 v}{\partial y^2}\right)(x_0)$ $f_4 = \frac{\partial^4 v}{\partial x^4}(x_N) = b(x_N) - \frac{\partial^4 v}{\partial y^4}(x_N) - 2\frac{\partial^2}{\partial x^2}\left(\frac{\partial^2 v}{\partial y^2}\right)(x_N)$

Table 3: Problem 1, simply-supported thin plate: A comparison of the condition number and the accuracy between CDF and PIF. Both methods use the same discretizations and they result in the systems of algebraic equations of the same number of unknowns. The order of accuracy is measured for the first five sets. $N = N_x = N_y$; $a(b) : a \times 10^b$.

$N+1$	Conditioning		$N_e(u)$		$N_e(v)$	
	CDF	PIF	CDF	PIF	CDF	PIF
6	1.66(1)	1.77(1)	2.71(-2)	5.53(-3)	5.54(-2)	1.10(-2)
8	5.41(1)	5.14(1)	5.74(-4)	7.25(-5)	8.12(-4)	1.33(-4)
10	1.39(2)	1.24(2)	1.02(-5)	7.19(-7)	1.30(-5)	9.84(-7)
12	3.02(2)	2.60(2)	1.31(-7)	6.39(-9)	1.59(-7)	7.78(-9)
14	5.81(2)	4.89(2)	1.29(-9)	4.60(-11)	1.52(-9)	5.27(-11)
16	1.02(3)	8.49(2)	1.01(-11)	2.74(-13)	1.17(-11)	3.03(-13)
18	1.67(3)	1.38(3)	6.44(-14)	3.13(-15)	7.51(-14)	4.15(-15)
20	2.60(3)	2.13(3)	3.92(-15)	2.62(-15)	9.28(-15)	3.86(-15)
			$O(N^{-17.38})$	$O(N^{-19.24})$	$O(N^{-17.94})$	$O(N^{-19.88})$

Table 4: Problem 2, clamped thin-plate: A comparison of the condition number and the accuracy between CDF and PIF. Both methods use the same discretizations and they result in the systems of algebraic equations of the same number of unknowns. The order of accuracy is measured for the first five sets. $N = N_x = N_y$; NRT: node-reduction technique; and IKT: kernel technique.

$N+1$	Conditioning			$N_e(v)$		
	CDF		PIF	CDF		PIF
	NRT	IKT		NRT	IKT	
6	4.40(2)	1.56(2)	1.68(2)	1.70(-1)	3.44(-2)	2.12(-2)
8	3.60(3)	1.67(3)	1.50(3)	1.92(-2)	3.32(-4)	1.31(-4)
10	2.02(4)	1.09(4)	8.85(3)	8.62(-4)	3.90(-6)	8.39(-7)
12	9.21(4)	5.11(4)	3.89(4)	2.24(-5)	3.80(-8)	5.27(-9)
14	3.48(5)	1.87(5)	1.37(5)	3.91(-7)	3.04(-10)	2.97(-11)
16	1.11(6)	5.75(5)	4.12(5)	4.92(-9)	2.03(-12)	1.97(-13)
18	3.14(6)	1.54(6)	1.08(6)	4.72(-11)	2.35(-13)	5.50(-14)
20	7.93(6)	3.71(6)	2.59(6)	3.86(-12)	2.54(-13)	5.18(-14)
				$O(N^{-13.36})$	$O(N^{-19.13})$	$O(N^{-21.10})$

Table 5: Problem 3, first-kind biharmonic problem, non-homogeneous boundary conditions: A comparison of accuracy and convergence between CDF and PIF. Both methods use the same discretizations and they result in the systems of algebraic equations of the same number of unknowns. The order of accuracy is measured for the first eight sets. $N = N_x = N_y$.

$N+1$	$N_e(v)$	
	DF	IF
6	1.39(0)	8.25(-1)
8	3.48(-1)	5.03(-2)
10	6.78(-2)	1.71(-3)
12	6.92(-3)	5.33(-5)
14	4.78(-4)	1.54(-6)
16	2.40(-5)	3.88(-8)
18	9.19(-7)	8.37(-10)
20	2.76(-8)	1.55(-11)
22	6.87(-10)	2.67(-12)
24	2.96(-10)	4.21(-12)
	$O(N^{-13.02})$	$O(N^{-18.42})$

a) one-dimensional domain

b) two-dimensional domain

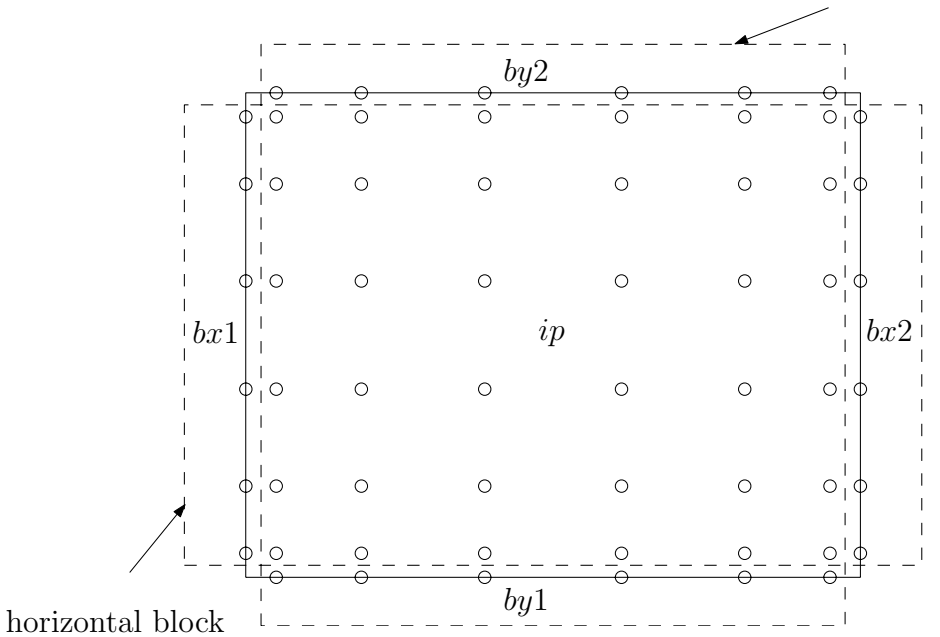

Figure 1: Geometry and discretization. ip: interior points; bx, by: boundary points.

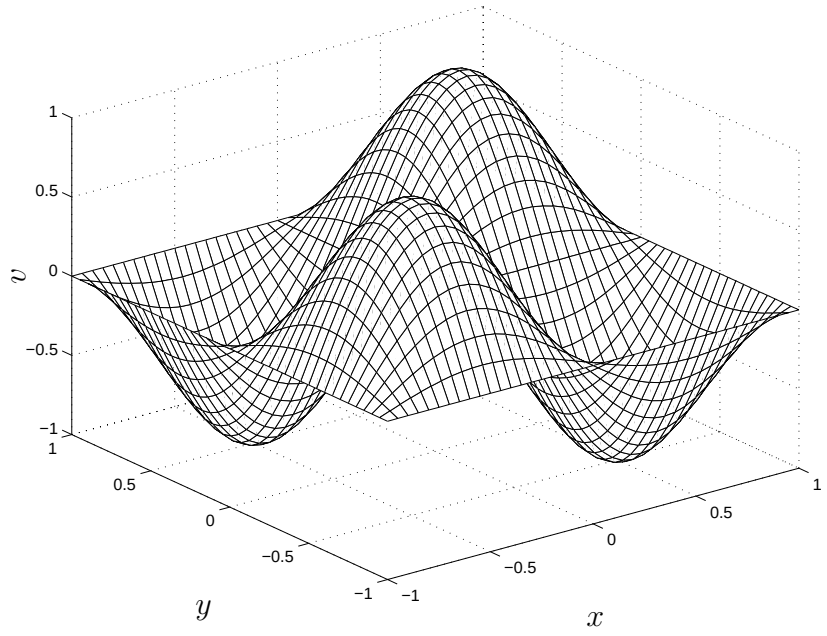

Figure 2: Problem 1: exact solution.

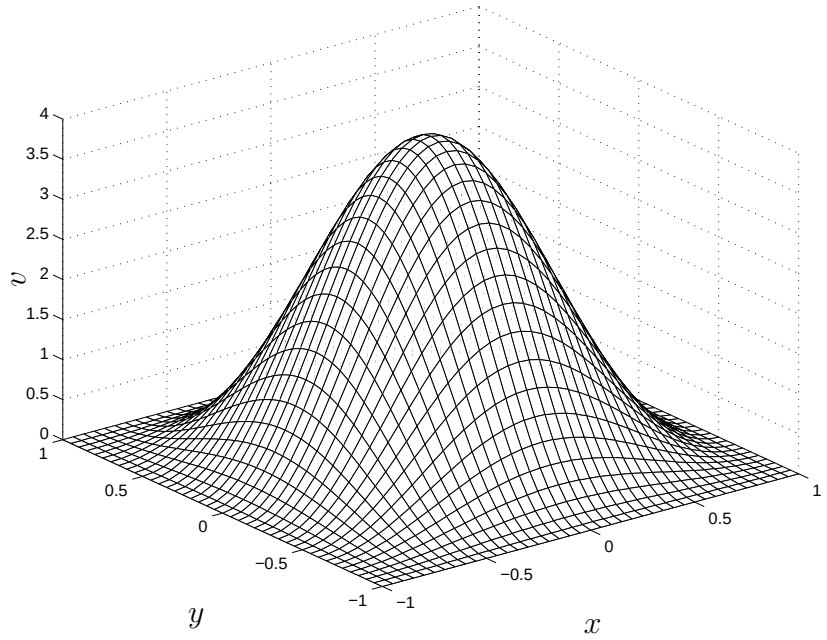

Figure 3: Problem 2: exact solution.

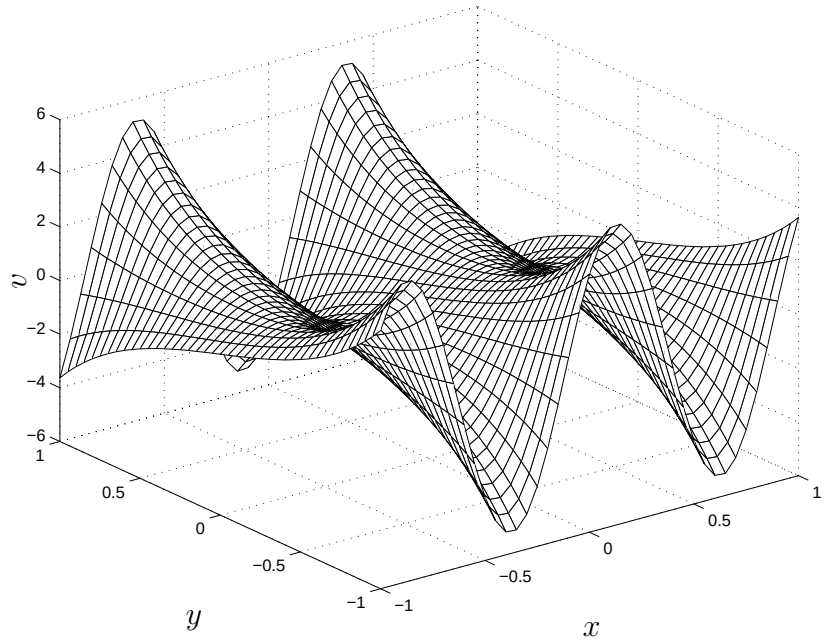

Figure 4: Problem 3: exact solution.